DOI: 10.32615/ps.2020.063 PHOTOSYNTHETICA 58 (5): 1098-1106, 2020

Ginkgo biloba and *Helianthus annuus* show different strategies to adjust photosynthesis, leaf water relations, and cell wall composition under water deficit stress

M. ROIG-OLIVER[+,†], M. NADAL[†], J. BOTA, and J. FLEXAS

Research Group on Plant Biology under Mediterranean Conditions, Department of Biology, Universitat de les Illes Balears (UIB), INAGEA, Carretera de Valldemossa Km 7.5, 07122 Palma, Illes Balears, Spain

Abstract

Cell wall thickness (T_{cw}) determines photosynthesis and leaf elasticity. However, only a few studies in angiosperms addressed cell wall composition implication in regulating photosynthesis and leaf water relations through mesophyll conductance (g_m) and bulk modulus of elasticity (ε) adjustments, respectively. Thus, we compared the phylogenetically distant *Ginkgo biloba* L. and *Helianthus annuus* L. under control and water deprivation to study the relationship between changes in cell wall composition (cellulose, hemicelluloses, and pectins) with g_m and ε. Although no changes were found for T_{cw}, both species differently modified cell wall composition, resulting in different physiological consequences. *H. annuus* increased cellulose, hemicelluloses, and pectins in a similar proportion, maintaining ε. Additionally, it reduced photosynthesis due to stomatal closure. *G. biloba* did not decrease photosynthesis and largely increased hemicelluloses, leaf mass area, and leaf density, enhancing ε. Nonetheless, no association between cell wall composition and g_m was found in either of the two species.

Keywords: angiosperm; gymnosperm; leaf structure.

Introduction

Photosynthesis is a complex phenomenon that involves both diffusional and biochemical processes (Flexas *et al*. 2004, von Caemmerer *et al*. 2009). The diffusional process consists of the CO_2 pathway from the atmosphere to the substomatal cavity (stomatal conductance, g_s) across the mesophyll tissue (mesophyll conductance, g_m) until reaching its carboxylation sites at chloroplasts stroma, where biochemical processes occur (Flexas *et al*. 2004, Evans *et al*. 2009, von Caemmerer *et al*. 2009). Even though the mechanistic nature of g_m is not yet fully understood (Evans *et al*. 2009, Flexas *et al*. 2012), some studies have evidenced that leaf anatomical traits, particularly cell wall thickness (T_{cw}) and chloroplasts surface area exposed to intercellular air spaces per leaf area (S_c/S), are crucial to determine g_m across plants' phylogeny and in response to different environmental conditions (Terashima *et al*. 2001, Evans *et al*. 2009, Flexas *et al*. 2012, Tomás *et al*. 2013, Carriquí *et al*. 2015, 2019, 2020; Tosens *et al*. 2016, Onoda *et al*. 2017, Peguero-Pina *et al*. 2017, Veromann-Jürgenson *et al*. 2017). Hence, as thick cell walls limit g_m and, simultaneously, potentially increase cells rigidity (enhanced bulk modulus of elasticity, ε) (Tyree and Jarvis 1982, Peguero-Pina *et al*. 2017), a trade-off between g_m and net photosynthetic rate (P_N) with ε was demonstrated in a wide range of species under nonstress conditions (Nadal *et al*. 2018). Nonetheless, the mechanistic basis of ε and its intraspecific dynamics during plant's acclimation to changing environmental conditions are still poorly understood. Although Niinemets (2001) and Sack *et al*. (2003) proposed that leaf structure, particularly leaf mass

Received 29 June 2020, *accepted* 27 August 2020.
[+]Corresponding author; e-mail: margaroig93@gmail.com
Abbreviations: a_f – apoplastic water fraction; AIR – alcohol insoluble residue; C^*_{ft} – leaf area specific capacitance at full turgor; ETR – electron transport rate; f_{ias} – fraction of mesophyll intercellular air spaces; g_m – mesophyll conductance; g_s – stomatal conductance; LA – leaf area; LD – leaf density; LMA – leaf mass area; P_N – net photosynthetic rate; R_{light} – light respiration; RWC_{tlp} – relative water content at turgor loss point; S_c/S – chloroplasts surface area exposed to intercellular air spaces per leaf area; T_{cw} – cell wall thickness; WUE_i – intrinsic water-use efficiency; ε – bulk modulus of elasticity; π_o – osmotic potential at full turgor; Ψ_{tlp} – water potential at turgor loss point.
Acknowledgments: This work was supported by the project PGC2018-093824-B-C41 from the Ministerio de Ciencia, Innovación y Universidades (Spain), the ERDF, the UE and the AEI. M. Roig-Oliver and M. Nadal were supported by predoctoral fellowships FPU16/01544 and BES-2015-072578, respectively, from Ministerio de Economía y Competitividad (MINECO, Spain). Additionally, M. Nadal was co-supported by the European Social Fund. We thank Dr. María José Clemente-Moreno for her advice in results analyses and María Teresa Mínguez (Universitat de València, Secció de Microscòpia Electrònica – SCSIE) and Dr. Ferran Hierro (Universitat de les Illes Balears, Serveis Cientificotècnics) for technical support during microscopic analyses. We also thank Mr. Miquel Truyols and collaborators of the UIB Experimental Field and Glasshouses that are supported by the UIB Grant 15/2015.
[†]Both authors contributed equally to this paper.

area (LMA) and leaf density (LD), was the main driver of ε, more recent studies suggested that cell wall composition and properties could be also relevant for determining ε (Moore *et al*. 2008, Solecka *et al*. 2008, Álvarez-Arenas *et al*. 2018, Roig-Oliver *et al*. 2020).

The plant cell wall, a complex structure considered as a protective barrier to face those biotic and abiotic stresses occurring during plants' life, is mainly compounded by cellulose microfibrils (Carpita and Gibeaut 1993, Cosgrove 1997, 2005; Somerville *et al*. 2004, Sarkar *et al*. 2009, Tenhaken 2015, Houston *et al*. 2016, Rui and Dinnery 2019). Between those closely packed microfibrils, noncellulosic neutral sugars (hereafter 'hemicelluloses') are placed, conferring stability to the wall (Carpita and Gibeaut 1993, Cosgrove 1997, 2005; Somerville *et al*. 2004, Sarkar *et al*. 2009, Tenhaken 2015, Rui and Dinnery 2019). This cellulose–hemicelluloses network is embedded in a pectin matrix which has been proposed as a crucial structure to maintain an appropriate cell wall hydric status, especially during water deficit stress (Vicré *et al*. 2004, Cosgrove 2005, Leucci *et al*. 2008, Moore *et al*. 2008, 2013; Schiraldi *et al*. 2012, Le Gall *et al*. 2015, Houston *et al*. 2016). Additionally, the pectin matrix seems to be a key structure determining wall porosity and thickness (Somerville *et al*. 2004, Cosgrove 2005, Tenhaken 2015, Houston *et al*. 2016, Rui and Dinnery 2019), leading to the suggestion that it could influence CO_2 diffusion and, thus, photosynthesis. However, only a few studies directly focused on the relationship between modifications in cell wall components and g_m (Ellsworth *et al*. 2018, Clemente-Moreno *et al*. 2019, Carriquí *et al.* 2020, Roig-Oliver *et al*. 2020). Particularly, Ellsworth *et al*. (2018) provided first evidence on how g_m reductions could be attributed to anatomical alterations due to cell wall changes testing *cslf6* rice mutants. Then, Clemente-Moreno *et al*. (2019) specifically identified pectins and/or the ratio of hemicelluloses to pectins as main drivers of g_m changes in *Nicotiana sylvestris* subjected to different environmental conditions. The relationship between modified cell wall composition and g_m changes could not be exclusively attributed to pectins as Roig-Oliver *et al*. (2020) showed that only cellulose correlated with g_m in *Vitis vinifera* cv. Grenache acclimated to contrasting conditions. Nonetheless, at an interspecific level and under nonstress conditions, the ratio of pectins to cellulose and hemicelluloses determined g_m in conifers (Carriquí *et al*. 2020). Thus, it appears that the relationship between cell wall main composition and g_m could be species-dependent (Roig-Oliver *et al*. 2020) and could be attributed to specific growing conditions.

Some studies have determined that cell wall composition differs among plants belonging to different phylogenetic groups (Popper and Fry 2004, Sørensen *et al*. 2010, Popper *et al*. 2011, Bartels and Classen 2017). Additionally, several studies have characterized cell wall composition changes in different monocot and dicot species under stressing conditions (*see*, for instance, Sweet *et al*. 1990, Vicré *et al*. 1999, 2004; Leucci *et al*. 2008, Moore *et al*. 2008, Solecka *et al*. 2008, Suwa *et al*. 2010, Carvalho *et al*. 2013, Baldwin *et al*. 2014, Zheng *et al*. 2014, Clemente-Moreno *et al*. 2019, Roig-Oliver *et al*. 2020). However, to our knowledge, no information is known regarding stress-induced changes in cell wall properties in other plant groups. Moreover, how these differences in cell wall composition in response to stress could be linked to differed strategies to regulate photosynthesis, leaf water relations and anatomical adjustments remain to be elucidated. In the current study, we compared the gymnosperm living fossil *Ginkgo biloba* L. (Ginkgoaceae) and the herbaceous angiosperm *Helianthus annuus* L. (Asteraceae) acclimated to two different experimental conditions (well-watered, *i.e*., control, and water deficit stress) to induce changes in cell wall composition that could influence photosynthesis, anatomical and/or leaf water relations responses.

Materials and methods

Plant material and growth conditions: One-year-old *G. biloba* plants were acquired from a garden center in horticultural alveolus. *H. annuus* seeds were individually sewed in horticultural alveolus using a mixture of 3:1 substrate:perlite. All plants were placed in a growth chamber at 22°C with 12/12-h light/darkness daily fluctuation receiving PPDF of 200–300 μmol m^{-2} s^{-1}. Water irrigation was assessed every two days to ensure plant growth. Three weeks later, when all plants had fully-developed leaves, they were transplanted to 3-L pots containing a mixture of 2:2 and 3:1 substrate:perlite for *G. biloba* and *H. annuus*, respectively. At this moment, six individual replicates per species were randomly subjected to two treatments: control (*i.e.*, well-watered) and water deficit stress. Water-stressed plants were monitored every two days to maintain pots field capacity at 50% by replacing evapotranspired water and control plants were daily irrigated to keep field capacity at 100%. To identify the onset of new leaves during plants' acclimation to experimental conditions, already emerged ones were labeled. In both cases, treatments lasted 40 d. All measurements were performed in new fully developed leaves developed under control or water-stressed conditions.

Gas-exchange and fluorescence measurements: At the end of the treatments, simultaneous measurements of gas exchange and chlorophyll *a* fluorescence with an open infrared gas-exchange system coupled with a 2-cm^2 fluorescence chamber (*Li-6400-40XT*, *Li-Cor Inc*., Lincoln, NE, USA) were performed in one leaf per plant in each species and treatment. Measurements were performed at saturating PPFD (1,500 μmol m^{-2} s^{-1} for *H. annuus*; 1,250 μmol m^{-2} s^{-1} for *G. biloba*; 90/10% of red/blue light, respectively, in both cases), 25°C block temperature, and 300 μmol min^{-1} flow rate. All gas-exchange measurements were corrected for CO_2 leakage in the leaf-gasket interface (Flexas *et al*. 2007). P_N, g_s, substomatal CO_2 concentration (C_i), and photochemical yield of PSII (Φ_{PSII}) were recorded after steady-state conditions were reached (15–30 min) at ambient CO_2 concentration (C_a) of 400 μmol mol^{-1}. P_N–C_i response curves were then performed by changing C_a in 14 steps (3–4 min), from 50 to 1,500 μmol(CO_2) mol^{-1}(air). Light curves under nonphotorespiratory conditions (1%

O_2) were performed to determine light respiration (R_{light}) and the PPFD fraction harvested by PSII (s) (Yin *et al*. 2009, 2011; Bellasio *et al*. 2016). From previous parameters, the electron transport rate (ETR) was calculated as described in Bellasio *et al*. (2016). The CO_2-compensation point in the absence of respiration (Γ^*) for *G. biloba* and *H. annuus* were obtained from comparing P_N–C_i curves under ambient (21%) and low O_2 (1%) conditions as described in Bellasio *et al*. (2016). Finally, mesophyll conductance (g_m) was determined by the curve-fitting method (Sharkey 2016) using R_{light} as an input and the Rubisco kinetics (K_c, K_o) from tobacco (Bernacchi *et al*. 2002). The mean Γ^* value obtained for each species under well-watered conditions was used for water-stressed plants as *in vivo* methods are not reliable under stress (Galmés *et al*. 2006).

Anatomical measurements: A portion of the leaves used for gas-exchange measurements were cut in small pieces avoiding main foliar structures to be fixed under vacuum pressure using glutaraldehyde 4% and paraformaldehyde 2% prepared in 0.01 M phosphate buffer (pH 7.4). Samples were post-fixed in 2% buffered osmium tetroxide for two hours and dehydrated by a graded ethanol series. The obtained pieces were embedded in *LR White* resin (*London Resin Company*) and placed in an oven at 60°C for 48 h (Tomás *et al*. 2013).

Semi-fine (0.8 µm) and ultra-fine (90 nm) cross-sections were cut using an ultramicrotome (*Leica UC6*, Vienna, Austria). Semi-fine sections were dyed with 1% toluidine blue to be viewed in a bright field with an *Olympus BX60* optic microscope. Pictures at 200× magnifications were taken with a digital camera (*U-TVO.5XC*, *Olympus*, Tokyo, Japan) to determine the fraction of mesophyll intercellular air spaces (f_{ias}). Ultra-fine sections for transmission electron microscopy (*TEM H600*, *Hitachi*, Tokyo, Japan) were contrasted with uranyl acetate and lead citrate to obtain pictures at 1,500× and 30,000× magnifications. The chloroplasts surface area exposed to intercellular air spaces per leaf area (S_c/S) and the cell wall thickness (T_{cw}) were measured from ultra-fine images at 1,500× and 30,000× magnifications, respectively. A cell curvature correction factor was determined according to Thain (1983) making an average length/width ratio of five randomly selected cells from both palisade and spongy mesophyll types for S_c/S estimation. Final values for measured parameters were obtained as an average of ten measurements from randomly selected cell structures using the *ImageJ* software (Wayne Rasband/NIH, Bethesda, MD, USA).

Cell wall extraction and fractionation: The same leaves used for gas exchange and anatomy sampling were kept under dark conditions overnight to minimize starch content. The following morning, around 1 g of fresh leaf tissue per plant was cut in small pieces and they were placed in glass tubes containing absolute ethanol (1:10, w/v). They were boiled until bleached and cleaned twice with acetone > 95% obtaining the alcohol insoluble residue (AIR), an approximation of the total isolated cell wall content. After dried, samples were grounded and starch remains were removed with α-amylase digestion. Then, three analytical replicates of each AIR weighting 3 mg were taken to be hydrolyzed with 2 M trifluoroacetic acid for an hour at 121°C. They were centrifuged at 13,000 × g for the obtention of two phases: the supernatant (noncellulosic cell wall components) and the pellet (cellulosic cell wall components). Whilst the supernatant was kept at –20°C to quantify hemicelluloses and uronic acids (*i.e*., pectins), the pellet was cleaned twice with distilled water and acetone > 95%. Once dried, pellets were hydrolyzed in 200 µl sulphuric acid 72% (w/v) for an hour, diluted to 6 ml with distilled water, and heated until degradation. Once cooled, the obtained aqueous samples were used for cellulose quantification. Cellulose and hemicellulose quantifications were determined following Dubois *et al*. (1956). Thus, samples absorbance was read at 490 nm and both sugars concentrations were estimated by interpolating sample values from a glucose calibration curve. Finally, pectin quantification was performed following Blumenkrantz and Asboe-Hansen (1973). Hence, samples absorbance was read at 520 nm and pectin content was calculated by interpolating sample values from a galacturonic acid calibration curve. In all cases, a *Multiskan Sky Microplate* spectrophotometer (*ThermoFisher Scientific*) was used.

Pressure-volume curves: A fully developed leaf neighboring the one used for the gas exchange was rehydrated with distilled water and kept under dark conditions overnight. The next morning, leaf water potential and mass were measured simultaneously to obtain pressure–volume (P–V) curves of, at least, ten points. Leaf water potential was determined using a pressure chamber (*Model 600D*, *PMS Instrument Company*, Albany, USA). From P–V curves analysis, leaf water potential at turgor loss point (Ψ_{tlp}), osmotic potential at full turgor (π_o), relative water content at turgor loss point (RWC_{tlp}), apoplastic water fraction (a_f), and leaf area specific capacitance at full turgor (C^*_{ft}) were obtained (Sack and Pasquet-Kok 2011). The bulk modulus of elasticity (ε) was determined using standardized major axes (SMA; Sack *et al*. 2003).

Leaf structure: The same leaves used for P–V curves were utilized to calculate the leaf mass area (LMA), the leaf density (LD), and the leaf area (LA) (Pérez-Harguindeguy *et al*. 2013). Leaves were rehydrated overnight and pictures of the LA including the petiole were analyzed with the *ImageJ* software (Wayne Rasband/NIH). Then, leaves were placed in an oven at 70°C for 72 h to obtain their dry mass. Leaf thickness was determined from six measurements per leaf avoiding main veins with a digital caliper. Thickness per area was used as a proxy to calculate LD.

Statistical analysis: Thompson test was performed to detect and eliminate outliers for all studied parameters. Two-way analysis of variance (*ANOVA*) and subsequent LSD test was assessed to determine significant (P<0.05) 'species' and 'treatments' effects and differences between groups, respectively. All analyses were performed using the *R* statistical software (*ver. 3.2.2*, *R Core Team*, Vienna, Austria).

Results

Physiological characterization: Under control conditions, *H. annuus* achieved the highest P_N and g_s [26.30 ± 2.27 μmol(CO_2) m^{-2} s^{-1} and 0.40 ± 0.06 mol(CO_2) m^{-2} s^{-1}, respectively], which were largely reduced under water deficit stress (Fig. 1*A*,*B*). Contrarily, *G. biloba* showed much lower assimilation under control conditions [7.91 ± 0.43 μmol(CO_2) m^{-2} s^{-1}], but neither P_N nor g_s experienced significant changes due to water deficit stress (Fig. 1*A*,*B*). Only *H. annuus* experienced an increase in WUE_i under water deficit stress conditions (Fig. 1*C*). Additionally, water-stressed *H. annuus* also showed reductions of both g_m (Fig. 1*D*) and ETR, the latter being also slightly reduced in *G. biloba* (Fig. 1*E*). Finally, R_{light} only revealed differences at P=0.053 for the 'treatments' effect as it slightly decreased under water deficit stress (Fig. 1*F*).

Leaf water relations: No treatment effect was detected for both Ψ_{tlp} and π_o (P=0.337 and 0.139, respectively) (Fig. 2*A*,*C*). Although RWC_{tlp} was maintained in *G. biloba*, it increased in water-stressed *H. annuus* in comparison to control (Fig. 2*B*). However, water-stressed *G. biloba* leaves were almost three-folds more rigid than control ones (61.17 ± 14.32 and 21.15 ± 2.36 MPa, respectively; Fig. 2*D*). Water deficit stress increased a_f and C^*_{ft} in *H. annuus* [0.55 ± 0.03 and 1.96 ± 0.25 mol(H_2O) m^{-2} MPa^{-1}, respectively], but no changes were detected in *G. biloba* (Fig. 2*E*,*F*).

Leaf structural and anatomical traits: Under water deficit stress conditions, *H. annuus* and *G. biloba* experienced an increase in both LMA and LD, being more marked in the latter species as they doubled control values (Table 1). An opposite pattern was found for LA, which decreased significantly under water deficit stress conditions, especially in *G. biloba* (Table 1). However, water deprivation did not significantly change anatomical parameters (*i.e.*, f_{ias}, S_c/S, and T_{cw}) in none of the two species (Table 1), which were evaluated from similar pictures to those from Fig. 3.

Leaf cell wall composition: Water deficit stress induced different changes in cell wall composition in the two species. *G. biloba* significantly increased hemicelluloses while slightly decreasing cellulose, with no changes in the total AIR and pectins (Table 2). Instead, *H. annuus* significantly enhanced the total AIR with also increased amounts of cellulose, hemicelluloses, and pectins in a similar proportion (Table 2).

Discussion

A classic response to water deficit stress involves a reduction of P_N associated to decreased leaf overall CO_2 diffusion (*i.e.*, g_s and g_m) (Chaves *et al*. 2002, 2008; Flexas *et al*. 2004, 2012; Nadal and Flexas 2019), which promotes enhanced WUE_i due to larger descents in g_s than in g_m (Flexas *et al.* 2013). In the current study, this pattern was only observed in water-stressed *H. annuus* plants as P_N, g_s, and g_m did not significantly decrease in *G. biloba*

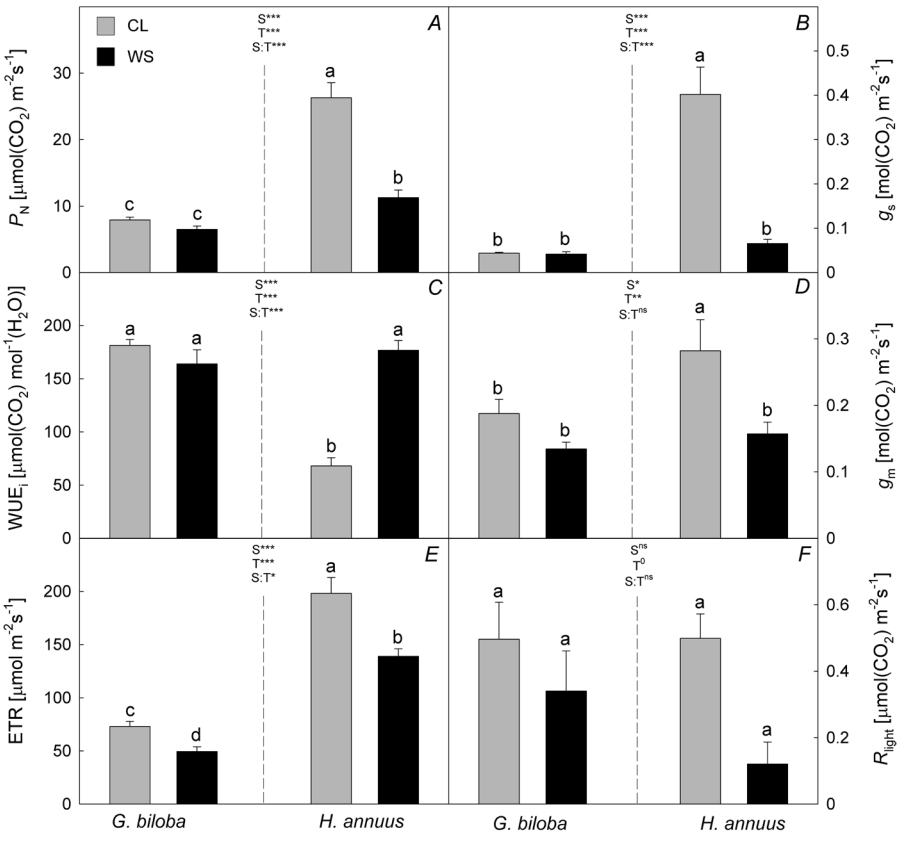

Fig. 1. (*A*) Net photosynthetic rate (P_N), (*B*) stomatal conductance (g_s), (*C*) intrinsic water-use efficiency (WUE_i), (*D*) mesophyll conductance (g_m), (*E*) electron transport rate (ETR), and (*F*) light respiration (R_{light}) in *Ginkgo biloba* and *Helianthus annuus* across conditions (CL – control, WS – water deficit stress). Species (S) and treatments (T) effects were quantified by two-way *ANOVA* and differences between groups were addressed by LSD test. *Different superscript letters* indicate significant differences. Significance: $^{***}P$<0.001; ** <0.01; * <0.05; ^{0} <0.1; ^{ns} >0.1. Values are means ± SE (n = 5–6).

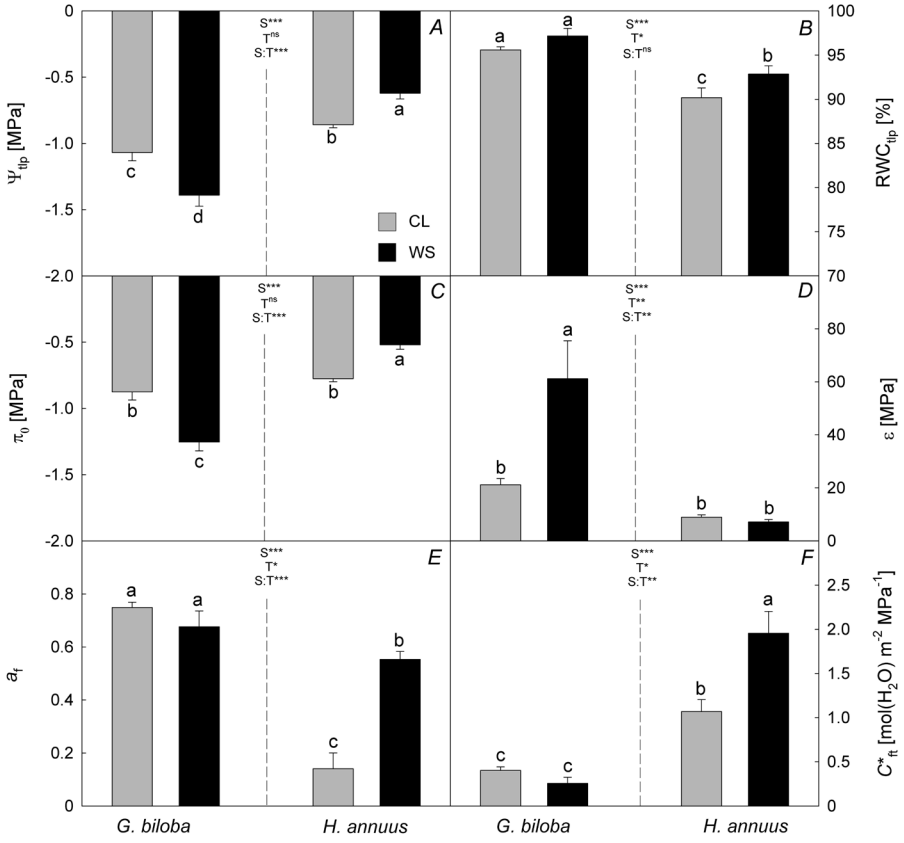

Fig. 2. (*A*) Water potential at turgor loss point (Ψ_{tlp}), (*B*) relative water content at turgor loss point (RWC_{tlp}), (*C*) osmotic potential at full turgor (π_o), (*D*) bulk modulus of elasticity (ε), (*E*) apoplastic water fraction (a_f), and (*F*) leaf area specific capacitance at full turgor (C^*_{ft}) in *Ginkgo biloba* and *Helianthus annuus* across conditions (CL – control, WS – water deficit stress). Species (S) and treatments (T) effects were quantified by two-way *ANOVA* and differences between groups were addressed by LSD test. Significance: $^{***}P<0.001$; ** <0.01; * <0.05; ^{0} <0.1; ^{ns} >0.1. Values are means ± SE (n = 5–6).

Table 1. Leaf structural and anatomical traits of *Ginkgo biloba* and *Helianthus annuus* across conditions (CL – control, WS – water deficit stress). Average values ± SE are shown for leaf mass area (LMA), leaf density (LD), leaf area (LA), fraction of mesophyll intercellular air spaces (f_{ias}), chloroplasts surface area exposed to intercellular air spaces per leaf area (S_c/S) and cell wall thickness (T_{cw}). Species and treatments effects were quantified by two-way *ANOVA* and differences between groups were addressed by LSD test. *Different superscript letters* indicate significant differences. n = 5–6.

Species and treatments	LMA [g m^{-2}]	LD [g cm^{-3}]	LA [cm^2]	f_{ias} [%]	S_c/S [m^2 m^{-2}]	T_{cw} [μm]
G. biloba – CL	41.42 ± 1.22^{bc}	0.15 ± 0.00^{c}	85.36 ± 8.34^{a}	30.87 ± 3.95^{b}	9.73 ± 1.28^{b}	0.39 ± 0.01^{a}
G. biloba – WS	89.52 ± 5.16^{a}	0.31 ± 0.02^{a}	21.50 ± 9.61^{c}	25.13 ± 1.83^{b}	10.92 ± 1.13^{b}	0.42 ± 0.03^{a}
H. annuus – CL	32.04 ± 0.71^{c}	0.16 ± 0.00^{c}	40.79 ± 6.03^{b}	45.50 ± 2.39^{a}	17.24 ± 1.48^{a}	0.18 ± 0.01^{b}
H. annuus – WS	48.18 ± 1.02^{b}	0.22 ± 0.00^{b}	21.37 ± 0.49^{c}	40.31 ± 0.58^{a}	18.74 ± 1.59^{a}	0.16 ± 0.01^{b}
Species	< 0.001	0.010	0.016	< 0.001	< 0.001	< 0.001
Treatments	< 0.001	< 0.001	< 0.001	0.058	0.347	0.708
Species:Treatments	< 0.001	< 0.001	< 0.001	0.921	0.914	0.177

(Fig. 1*A–D*). Despite opposite patterns for photosynthesis regulation under water deficit stress, both species modified their foliage structure (*i.e.*, increased LMA and LD, *see* Table 1) as previously reported by Niinemets *et al*. (2009). Additionally, water deficit stress strongly limited leaf development in both species as LA decreased significantly (Table 1), which has been described as a typical response to water deficit stress (Chaves *et al.* 2002). However, although Chartzoulakis *et al*. (2002) and Hafez *et al*. (2020) reported modifications in leaf, mesophyll, and epidermis thicknesses as well as in f_{ias} testing avocado and barley, respectively, under water deprivation, Tomás *et al.* (2014) did not detect strong subcellular anatomical alterations in water-stressed grapevine cultivars. In fact, in the present study neither T_{cw} nor other subcellular anatomical traits classically affecting g_m were modified under water deficit stress (Table 1), suggesting that decreased g_m in water-stressed *H. annuus* might be due to other nonstudied characteristics (*e.g.*, aquaporins and/or carbonic anhydrases, *see* Pérez-Martín *et al*. 2014).

Poorter *et al*. (2009) proposed that LD could reflect, to some extent, the cell wall content per leaf. Nonetheless, AIR variations only followed the same pattern as LD in *H. annuus*, as the slight increase detected in *G. biloba*

was not significant (Table 2). AIR enhancement due to water deficit stress was previously detected in *N. sylvestris* (Clemente-Moreno *et al*. 2019) and *V. vinifera* (Roig-Oliver *et al*. 2020). Concerning specific cell wall main composition, it has been reported that variations in cellulose content may depend, for instance, on species, specific plant tissues, plants' age, and/or level of water deficit (Sweet *et al*. 1990, Zheng *et al*. 2014, Clemente-Moreno *et al*. 2019, Roig-Oliver *et al*. 2020). Thus, cellulose increased in *H. annuus* as previously shown for other species (Sweet *et al*. 1990, Clemente-Moreno *et al*. 2019, Roig-Oliver *et al*. 2020), but slightly decreased in *G. biloba* (Table 2). However, hemicelluloses have been found to either increase (Vicré *et al*. 1999), decrease (Sweet *et al*. 1990, Roig-Oliver *et al*. 2020), or stay constant (Clemente-Moreno *et al*. 2019) after exposure to water deficit stress. In our study, both species, especially *G. biloba*, presented increased amounts of hemicelluloses under water deficit stress (Table 2). Finally, pectins usually increase during water deficit because they play a key role in adjusting cell wall flexibility, thus, controlling cell wall hydric status (Sweet *et al*. 1990, Vicré *et al*. 1999, 2004; Cosgrove 2005, Leucci *et al*. 2008, Moore *et al*. 2008, 2013; Le Gall *et al*. 2015, Tenhaken 2015, Houston *et al*. 2016, Clemente-Moreno *et al*. 2019, Rui and Dinnery 2019, Roig-Oliver *et al*. 2020). However, in our study pectins were only enhanced in water-stressed *H. annuus* in a similar proportion to cellulose and hemicelluloses (Table 2). Additionally, the potential importance of pectins in determining ε adjustments has already been proposed (Moore *et al*. 2008, Solecka *et al*. 2008, Niinemets 2016) and Roig-Oliver *et al*. (2020) provided empirical evidence for this in grapevines. Surprisingly, *H. annuus* maintained ε under water deficit stress, while *G. biloba* – having kept pectins constant – drastically enhanced leaves rigidity once subjected to water deficit stress (Fig. 2*D*) as usually reported for other species (Bowman and Roberts 1985, Lo Gullo and Salleo 1988, Abrams 1990, Kloeppel *et al*. 1994). Although more experimental conditions should be tested to set concluding statements, our results suggest that ε adjustments in water-stressed *G. biloba* could be much more related to changes in leaf structure (*i.e*., decreased LA and enhanced LMA and LD) and hemicelluloses rather than to other cell wall components. However, while increased ε and LD have been proposed to involve reductions in g_m (Niinemets *et al*. 2009, Nadal *et al*. 2018), *G. biloba* was able to maintain g_m at control values under water deficit stress conditions. Oppositely, *H. annuus* differed from the previous strategy as leaf structure and cell wall composition changes were not reflected in ε modifications. Instead, increased AIR, cellulose, hemicelluloses, and pectins under water deficit stress were reflected as an increase in a_f and C^*_{ft} (Fig. 2*E*, *F*).

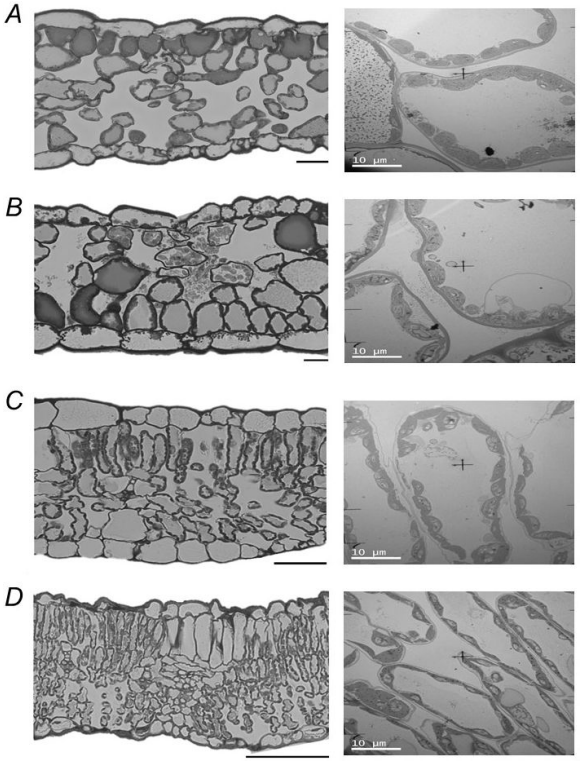

Fig. 3. Representative micrographs from semi-fine (*left*) and ultra-fine (*right*) cross-sections taken at 200× and at 1,500× magnifications, respectively, for *Ginkgo biloba* (*A*,*B*) and *Helianthus annuus* (*C*,*D*) under control and water deficit stress conditions, respectively. Black scale bars = 100 µm. Detailed quantitative analyses of studied anatomical parameters are reported in Table 1.

Table 2. Leaf cell wall composition of *Ginkgo biloba* and *Helianthus annuus* across conditions (CL – control, WS – water deficit stress). Average values ± SE are shown for alcohol insoluble residue (AIR), cellulose, hemicelluloses, and pectins contents. Species and treatments effects were quantified by two-way *ANOVA* and differences between groups were addressed by LSD test. *Different superscript letters* indicate significant differences. n = 5–6.

Species and treatments	AIR [g g^{-1}(DM)]	Cellulose [mg g^{-1}(AIR)]	Hemicelluloses [mg g^{-1}(AIR)]	Pectins [mg g^{-1}(AIR)]
G. biloba – CL	0.16 ± 0.03^{a}	125.2 ± 12.9^{a}	176.5 ± 18.3^{b}	71.27 ± 6.52^{b}
G. biloba – WS	0.19 ± 0.01^{a}	100.2 ± 11.6^{ab}	261.4 ± 30.6^{a}	79.60 ± 4.16^{b}
H. annuus – CL	0.09 ± 0.01^{b}	86.6 ± 8.8^{b}	79.7 ± 12.5^{c}	73.09 ± 12.09^{b}
H. annuus – WS	0.15 ± 0.01^{a}	128.7 ± 5.2^{a}	156.2 ± 9.8^{b}	103.68 ± 3.45^{a}
Species	< 0.001	0.622	< 0.001	0.051
Treatments	0.012	0.406	0.001	0.013
Species:Treatments	0.351	0.003	0.847	0.133

To our knowledge, this study provides the first evidence on how changes in cell wall main composition may play a role in determining different strategies to face water deficit stress by adjustments in ε and/or g_m testing species from different phylogenetic groups. Contrary to Clemente-Moreno *et al*. (2019) and Roig-Oliver *et al*. (2020), in the two species studied here, water deficit stress induced changes in cell wall composition that did not affect g_m and photosynthesis, but differently modified water relations parameters. Thus, more detailed studies using a larger range of species and treatments are required for a better understanding of how cell wall composition – including other cell wall compounds such as lignins and cell wall-bound phenolics – can involve changes in leaf physiology and to what extent these responses are species-dependent and/or change across plants phylogeny.

References

Abrams M.D.: Adaptations and responses to drought in *Quercus* species of North America. – Tree Physiol. **7***:* 227-238, 1990.

Álvarez-Arenas T.E.G., Sancho-Knapik D., Peguero-Pina J.J. *et al*.: Non-contact ultrasonic resonant spectroscopy resolves the elastic properties of layered plant tissues. – Appl. Phys. Lett. **113**: 253704, 2018.

Baldwin L., Domon J.M., Klimek J.F. *et al*.: Structural alteration of cell wall pectins accompanies pea development in response to cold. – Phytochemistry **104**: 37-47, 2014.

Bartels D., Classen B.: Structural investigations on arabino-galactan-proteins from a lycophyte and different monilophytes (ferns) in the evolutionary context. – Carbohydr. Polym. **172**: 342-351, 2017.

Bellasio C., Beerling D.J., Griffiths H.: An Excel tool for deriving key photosynthetic parameters from combined gas exchange and chlorophyll fluorescence: theory and practice. – Plant Cell Environ. **39**: 1180-1197, 2016.

Bernacchi C.J., Portis A.R., Nakano H. *et al*.: Temperature response of mesophyll conductance. Implications for the determination of Rubisco enzyme kinetics and for limitations to photosynthesis *in vivo*. – Plant Physiol. **130**: 1992-1998, 2002.

Blumenkrantz N., Asboe-Hansen G.: New method for quantitative determination of uronic acids. – Anal. Biochem. **54**: 484-489, 1973.

Bowman W.D., Roberts S.W.: Seasonal changes in tissue elasticity in chaparral shrubs. – Physiol. Plantarum **65***:* 233-236*, 1985.*

Carpita N.C., Gibeaut D.M.: Structural models of primary cell walls in flowering plants: consistency of molecular structure with the physical properties of the walls during growth. – Plant J. **3**: 1-30, 1993.

Carriquí M., Cabrera H.M., Conesa M.À. *et al*.: Diffusional limitations explain the lower photosynthetic capacity of ferns as compared with angiosperms in a common garden study. – Plant Cell Environ. **38**: 448-460, 2015.

Carriquí M., Nadal M., Clemente-Moreno M.J. *et al*.: Cell wall composition strongly influences mesophyll conductance in gymnosperms. – Plant J. **103**: 1372-1385, 2020.

Carriquí M., Roig-Oliver M., Brodribb T.J. *et al*.: Anatomical constraints to nonstomatal diffusion conductance and photosynthesis in lycophytes and bryophytes. – New Phytol. **222**: 1256-1270, 2019.

Carvalho C.P., Hayashi A.H., Braga M.R., Nievola C.C.: Biochemical and anatomical responses related to the in vitro survival of the tropical bromeliad *Nidularium minutum* to low temperatures. – Plant Physiol. Bioch. **71**: 144-154, 2013.

Chartzoulakis K., Patakas A., Kofidis G. *et al*.: Water stress affects leaf anatomy, gas exchange, water relations and growth of two avocado cultivars. – Sci. Hortic.-Amsterdam **95**: 39-50, 2002.

Chaves M.M., Flexas J., Pinheiro C.: Photosynthesis under drought and salt stress: regulation mechanisms from whole plant to cell. – Ann. Bot.-London **103**: 551-560, 2008.

Chaves M.M., Pereira J.S., Maroco J. *et al*.: How plants cope with water stress in the field. Photosynthesis and Growth. – Ann. Bot.-London **89**: 907-916, 2002.

Clemente-Moreno M.J., Gago J., Díaz-Vivancos P. *et al*.: The apoplastic antioxidant system and altered cell wall dynamics influence mesophyll conductance and the rate of photosynthesis. – Plant J. **99**: 1031-1046, 2019.

Cosgrove D.J.: Relaxation in a high-stress environment: the molecular bases of extensible cell walls and cell enlargement. – Plant Cell **9**: 1031-1041, 1997.

Cosgrove D.J.: Growth of the plant cell wall. – Nat. Rev. Mol. Cell Biol. **6**: 850-861, 2005.

Dubois M., Gilles K.A., Hamilton J.K. *et al*.: Colorimetric method for determination of sugars and related substances. – Anal. Chem. **28**: 350-356, 1956.

Ellsworth P.V., Ellsworth P.Z., Koteyeva N.K., Cousins A.B.: Cell wall properties in *Oryza sativa* influence mesophyll CO_2 conductance. – New Phytol. **219**: 66-76, 2018.

Evans J.R., Kaldenhoff R., Genty B., Terashima I.: Resistance along the CO_2 diffusion pathway inside leaves. – J. Exp. Bot. **60**: 2235-2248, 2009.

Flexas J., Barbour M.M., Brendel O. *et al*.: Mesophyll conductance to CO_2: an unappreciated central player in photosynthesis. – Plant Sci. **193-194**: 70-84, 2012.

Flexas J., Bota J., Loreto F. *et al*.: Diffusive and metabolic limitations to photosynthesis under drought and salinity in C_3 plants. – Plant Biol. **6**: 269-279, 2004.

Flexas J., Díaz-Espejo A., Berry J.A. *et al*.: Analysis of leakage in IRGA's leaf chambers of open gas exchange systems: quantification and its effects in photosynthesis parameterization. – J. Exp. Bot. **58**: 1533-1543, 2007.

Flexas J., Niinemets Ü., Gallé A. *et al*.: Diffusional conductances to CO_2 as a target for increasing photosynthesis and photosynthetic water-use efficiency. – Photosynth. Res. **117**: 45-59, 2013.

Galmés J., Medrano H., Flexas J.: Acclimation of Rubisco specificity factor to drought in tobacco: discrepancies between *in vitro* and *in vivo* estimations. – J. Exp. Bot. **57**: 3659-3667, 2006.

Hafez Y., Attia K., Alamery S. *et al*.: Beneficial effects of biochar and chitosan on antioxidative capacity, osmolytes accumulation, and anatomical characters of water-stressed barley plants. – Agronomy **10**: 630, 2020.

Houston K., Tucker M.R., Chowdhury J. *et al*.: The plant cell wall: a complex and dynamic structure as revealed by the responses of genes under stress conditions. – Front. Plant Sci. **7**: 984, 2016.

Kloeppel B.D., Kubiske M.E., Abrams *M.D.:* Seasonal tissue water relations of four successional Pennsylvania barrens species in open and understory environments. – Int. J. Plant Sci. **155***:* 73-79*, 1994.*

Le Gall H., Philippe F., Domon J.M. *et al*.: Cell wall metabolism in response to abiotic stress. – Plants-Basel **4**: 112-166, 2015.

Leucci M.R., Lenucci M.S., Piro G., Dalessandro G.: Water stress and cell wall polysaccharides in the apical root zone of wheat cultivars varying in drought tolerance. – J. Plant Physiol. **165**: 1168-1180, 2008.

Lo Gullo M.A., Salleo S.: Different strategies of drought

resistance in three Mediterranean sclerophyllous trees growing in the same environmental conditions. – New Phytol. **108**: 267-276, 1988.

Moore J.P., Farrant J.M., Driouich A.: A role for pectin-associated arabinans in maintaining the flexibility of the plant cell wall during water deficit stress. – Plant Signal. Behav. **3**: 102-104, 2008.

Moore J.P., Nguema-Ona E.E., Vicré-Gibouin M. *et al*.: Arabinose-rich polymers as an evolutionary strategy to plasticize resurrection plant cell walls against desiccation. – Planta **237**: 739-754, 2013.

Nadal M., Flexas J.: Variation in photosynthetic characteristics with growth form in a water-limited scenario: Implications for assimilation rated and water use efficiency in crops. – Agr. Water Manage. **216**: 457-472, 2019.

Nadal M., Flexas J., Gulías J.: Possible link between photosynthesis and leaf modulus of elasticity among vascular plants: A new player in leaf traits relationships? – Ecol. Lett. **21**: 1372-1379, 2018.

Niinemets Ü.: Global-scale climatic controls of leaf dry mass per area, density, and thickness in trees and shrubs. – Ecology **82**: 453-469, 2001.

Niinemets Ü.: Does the touch of cold make evergreen leaves tougher? – Tree Physiol. **36**: 267-272, 2016.

Niinemets Ü., Díaz-Espejo A., Flexas J. *et al*.: Role of mesophyll diffusion conductance in constraining potential photosynthetic productivity in the field. – J. Exp. Bot. **60**: 2249-2270, 2009.

Onoda Y., Wright I.J., Evans J.R. *et al*.: Physiological and structural tradeoffs underlying the leaf economics spectrum. – New Phytol. **214**: 1447-1463, 2017.

Peguero-Pina J.J., Sancho-Knapik D., Gil-Pelegrín E.: Ancient cell structural traits and photosynthesis in today's environment. – J. Exp. Bot. **68**: 1389-1392, 2017.

Pérez-Harguindeguy N., Díaz S., Garnier E. *et al*.: New handbook for standardised measurement of plant functional traits worldwide. – Aust. J. Bot. **61**: 167-234, 2013.

Pérez-Martín A., Michelazzo C., Torres-Ruiz J.M. *et al*.: Regulation of photosynthesis and stomatal and mesophyll conductance under water stress and recovery in olive trees: correlation with gene expression of carbonic anhydrase and aquaporins. – J. Exp. Bot. **65**: 3143-3156, 2014.

Poorter H., Niinemets Ü., Poorter L. *et al*.: Causes and consequences of variation in leaf mass per area (LMA): a meta-analysis. – New Phytol. **182**: 565-588, 2009.

Popper Z.A., Fry S.C.: Primary cell wall composition of pteridophytes and spermatophytes. – New Phytol. **164**: 165-174, 2004.

Popper Z.A., Michel G., Hervé C. *et al*: Evolution and diversity of plant cell walls: from algae to flowering plants. – Annu. Rev. Plant Biol. **62**: 567-590, 2011.

Roig-Oliver M., Nadal M., Clemente-Moreno M.J. *et al*.: Cell wall components regulate photosynthesis and leaf water relations of *Vitis vinifera* cv. Grenache acclimated to contrasting environmental conditions. – J. Plant Physiol. **244**: 153084, 2020.

Rui Y., Dinnery J.R.: A wall with integrity: surveillance and maintenance of the plant cell wall under stress. – New Phytol. **225**: 1428-1439, 2019.

Sack L., Cowan P.D., Jaikumar N., Holbrook N.M.: The 'hydrology' of leaves: coordination of structure and function in temperate woody species. – Plant Cell Environ. **26**: 1343-1356, 2003.

Sack L., Pasquet-Kok J.: Leaf pressure-volume curve parameters. PrometheusWiki contributors, 2011. *Available at*: http://prometheuswiki.org/tiki-pagehistory.php?page=Leaf%20pressure-volume%20curve%20parameters&preview=16.

Sarkar P., Bosneaga E., Auer M.: Plant cell walls throughout evolution: towards a molecular understanding of their design principles. – J. Exp. Bot. **60**: 3615-3635, 2009.

Schiraldi A., Fessas D., Signorelli M.: Water activity in biological systems – A review. – Pol. J. Food Nutr. Sci. **62**: 5-13, 2012.

Sharkey T.D.: What gas exchange data can tell us about photosynthesis. – Plant Cell Environ. **39**: 1161-1163, 2016.

Solecka D., Zebrowski J., Kacperska A.: Are pectins involved in cold acclimation and de-acclimation of winter oil-seed rape plants? – Ann. Bot.-London **101**: 521-530, 2008.

Somerville C., Bauer S., Brinistool G. *et al*.: Toward a systems approach to understanding plant cell walls. – Science **306**: 2206-2211, 2004.

Sørensen I., Domozych D., Williats W.G.T.: How have plant cell walls evolved? – Plant Physiol. **153**: 366-372, 2010.

Suwa R., Hakata H., Hara H. *et al*.: High temperature effects on photosynthate partitioning and sugar metabolism during ear expansion in maize (*Zea mays* L.) genotypes. – Plant Physiol. Bioch. **48**: 124-130, 2010.

Sweet W.J., Morrison J.C., Labavitch J.M., Matthews M.A.: Altered synthesis and composition of cell wall of grape (*Vitis vinifera* L.) leaves during expansion and growth inhibiting water deficit. – Plant Cell Physiol. **31**: 407-414, 1990.

Tenhaken R.: Cell wall remodelling under abiotic stress. – Front. Plant Sci. **5**: 771, 2015.

Terashima I., Miyazawa S.I., Hanba Y.T.: Why are sun leaves thicker than shade leaves? Consideration based on analyses of CO_2 diffusion in the leaf. – J. Plant Res. **114**: 93-105, 2001.

Thain J.F.: Curvature correlation factors in the measurements of cell surface areas in plant tissues. – J. Exp. Bot. **34**: 87-94, 1983.

Tomás M., Flexas J., Copolovici L. *et al*.: Importance of leaf anatomy in determining mesophyll diffusion conductance to CO_2 across species: quantitative limitations and scaling up by models. – J. Exp. Bot. **64**: 2269-2281, 2013.

Tomás M., Medrano H., Brugnoli E. *et al*.: Variability of mesophyll conductance in grapevine cultivars under water stress conditions in relation to leaf anatomy and water use efficiency. – Aust. J. Grape Wine Res. **20**: 272-280, 2014.

Tosens T., Nishida K., Gago J. *et al*.: The photosynthetic capacity in 35 ferns and fern allies: mesophyll CO_2 diffusion as a key trait. – New Phytol. **209**: 1576-1590, 2016.

Tyree M.T., Jarvis P.G.: Water in tissues and cells. – In: Lange O.L., Nobel P.S., Osmond C.B., Ziegler H. (ed.): Physiological Plant Ecology II. Encyclopedia of Plant Physiology (New Series). Pp. 35-77. Springer Verlag, Berlin-Heidelberg 1982.

Veromann-Jürgenson L.L., Tosens T., Laanisto L., Niinemets Ü.: Extremely thick cell walls and low mesophyll conductance: welcome to the world of ancient living! – J. Exp. Bot. **68**: 1639-1653, 2017.

Vicré M., Lerouxel O., Farrant J. *et al*.: Composition and desiccation-induced alterations of the cell wall in the resurrection plant *Craterostigma wilmsii*. – Physiol. Plantarum **120**: 229-239, 2004.

Vicré M., Sherwin H.W., Driouich A. *et al*.: Cell wall characteristics and structure of hydrated and dry leaves of the resurrection plant *Craterostigma wilmsii*, a microscopical study. – J. Plant Physiol. **155**: 719-726, 1999.

von Caemmerer S., Farquhar G., Berry J. *et al*.: Biochemical model of C_3 photosynthesis. – In: Laisk A., Nedbal L., Govindjee (ed.): Photosynthesis in Silico: Understanding Complexity from Molecules to Ecosystems. Pp. 209-230. Springer, Dordrecht 2009.

Yin X., Struik P.C., Romero P. *et al*.: Using combined measurements of gas exchange and chlorophyll fluorescence to estimate parameters of a biochemical C_3 photosynthesis

model: a critical appraisal and a new integrated approach applied to leaves in a wheat (*Triticum aestivum*) canopy. – Plant Cell Environ. **32**: 448-464, 2009.

Yin X., Sun Z., Struik P.C., Gu J.: Evaluating a new method to estimate the rate of leaf respiration in the light by analysis of combined gas exchange and chlorophyll fluorescence measurements. – J. Exp. Bot. **62**: 3489-3499, 2011.

Zheng M., Meng Y., Yang C. *et al.*: Protein expression changes during cotton fibre elongation in response to drought stress and recovery. – Proteomics **14**: 1776-1795, 2014.